JOURNAL OF MATERIALS SCIENCE 35 (2000) 1773–1785

Submicron diameter nickel filaments and their polymer-matrix composites

XIAOPING SHUI, D. D. L. CHUNG
Composite Materials Research Laboratory, State University of New York at Buffalo, Buffalo, NY 14260-4400, USA

Discontinuous nickel filaments of diameter 0.4 μm and having a carbon core of diameter 0.1 μm were fabricated by electroplating nickel on discontinuous carbon filaments. They exhibited a grain size of 0.016 μm and electrical resistivity of about 5×10^{-6} Ω·cm. In an amount as low as 7 vol.% in a polymer (polyether sulfone) matrix, they resulted in a composite exhibiting electromagnetic interference shielding effectiveness of 87 dB and reflection coefficient 0.95 at 1–2 GHz, tensile strength 52 MPa, tensile ductility 1.0%, and density 1.87 g/cm^3. © *2000 Kluwer Academic Publishers*

1. Introduction

Metal wires/fibers are conventionally made by either metal forming (such as wire drawing) or melt spinning. Both processes become more difficult as the fiber diameter decreases. Thus, the use of these processes to make fibers of diameter a few micrometers or less is expensive and difficult. As a result, metal fibers of diameter less than about 2 μm are essentially not available. By using a totally different process, which is inexpensive, we have fabricated submicron diameter nickel filaments [1, 2]. This process involves electroplating nickel on carbon filaments of diameter 0.1 μm, so that the resulting filament has diameter 0.4 μm. As nickel constitutes 94% of the volume of the coated filament, the coated filament is referred to as a nickel filament. The electroplating of nickel or copper has been previously performed on conventional carbon fibers (diameter 7 μm), such that the coating thickness is much smaller than the original fiber diameter [3–5]. Electroplating on the 0.1 μm diameter carbon filaments, which are discontinuous (length > 100 μm), is much more challenging than electroplating on continuous 7 μm diameter carbon fibers, since the discontinuous nature makes the application of electrical contacts intuitively difficult and the small diameter makes the filaments easy to break. This paper describes the process of making the nickel filaments.

Metal fibers/filaments of small diameter are technologically attractive for use as a filler in composite materials, such as polymer-matrix composites. The small diameter is particularly attractive for composites that are used for electromagnetic interference (EMI) shielding or for reflecting electromagnetic radiation in the radio wave and microwave regime, which is relevant to radars, wireless communication and electrostatic discharge protection. A high shielding effectiveness alleviates the problem of electronic pollution emanating from radio frequency wireless communication devices and other electronic equipment. A high reflectivity is attractive for use in microwave waveguides, electrostatic discharge protection and other radio wave or microwave devices. A small diameter is preferred for the metal filaments because of the skin effect, which refers to the phenomenon in which electromagnetic radiation at a high frequency interacts only with the near surface region of a conductor. Due to the skin effect, a composite with metal filaments of a smaller diameter is more effective than one with metal filaments of a larger diameter at the same volume fraction for shielding or reflection. This paper provides data which show that the submicron diameter nickel filaments are indeed very effective for these electromagnetic applications. In addition, this paper describes the mechanical properties of these composites. Comparative data (both electromagnetic and mechanical) are given for composites with the submicron diameter nickel filaments, those with commercial nickel fibers (a 20 μm diameter nickel fiber from National Standard Co., Corbin, Kentucky, and a 2 μm diameter nickel fiber from Ribtec, Inc., Gahanna, Ohio) and those with 0.1 μm diameter carbon filaments (the core of each nickel filament; type ADNH carbon filaments from Applied Sciences Inc., Cedarville, Ohio). In this work, "fibers" refer to those of diameter more than 1 μm and "filaments" refer to those of diameter less than 1 μm.

2. Nickel filaments

2.1. Nickel filament fabrication

The nickel filaments were fabricated by electroplating nickel on carbon filaments, which were made using methane as the primary source gas and an iron containing catalyst. During carbon filament growth, hydrogen sulfide was added to the feedstock in small amounts to increase the filament yield. The basic properties of carbon filaments, as provided by Applied Sciences Inc., are listed in Table I. The surface area in Table I was calculated, according to R. Alig of Applied Sciences Inc., by assuming that the fiber was a solid cylinder with a density of 2 g/cm^3. In reality, the filament is a microtube with the inner hole diameter varying from

TABLE I Properties of carbon filaments

Diameter (μm)	0.16
Surface area (m^2/g)	12.5
Bulk density (cm^3/g) (compressed)	1620
Surface chemistry	Nitrogen groups
Sizing	None
SEM morphology	Entwined mass
Density (g/cm^3)	2
Aspect ratio	50–200

approximately 20 to 75 nm, as shown by scanning electron microscopy (SEM).

The electroplating was conducted by using a nickel anode and a nickel sulfate electrolyte solution. The fabricating process included the following five steps.

(a) *Pre-treatment.* It is important to clean the surface of an object to be electroplated prior to electroplating. To cleanse, the filaments were immersed in acetone (contained in a beaker) and stirred for 10 min using a stirring plate. This caused the acetone to change in appearance, from clear to yellow, indicating the cleansing action of the medium. Then the filaments were separated from acetone by vacuum infiltration. This was repeated three times or until the acetone became clear. After filtration, the filaments were allowed to air dry. The cleansing removed a tarry substance which comprised mainly polyaromatic hydrocarbons [6].

(b) *Dispersing.* After surface cleansing and drying in air, the filaments were immersed in distilled water in a blender for a few minutes. Then, the blender was operated at a low speed for 1 min. After that, the filaments were separated from the water by vacuum filtration. The filaments were then immersed in the electrolyte solution in the blender and blended for 0.5 min. The filaments were thus well dispersed in the electrolyte solution, such that bubbles were present along with the filaments. The bubbles were needed for making the filament mass float during electroplating.

(c) *Electroplating.* After dispersing, the filaments were floated on the top of the electrolyte. As shown in Fig. 1, a nickel plate, used as an anode, together with an electrical lead, was put into the bottom of a beaker. The lead was insulated from the cathode by a plastic tube. The cathode which was in contact with the filaments was a copper mesh. A Teflon coated stirrer was immersed in the middle of the beaker.

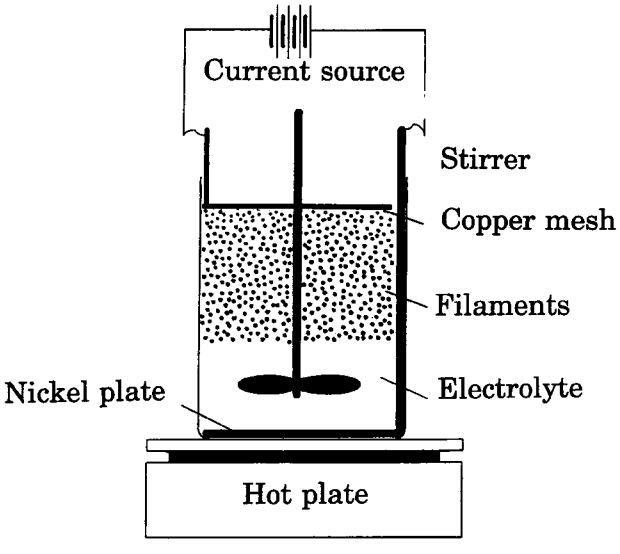

Figure 1 Illustration of the electroplating set-up.

For 1 g of carbon filaments, the cathode current was set at 16 A. Considering the huge surface area of the filaments, which was about 12.5 m^2 per gram of filaments, the electrical current density was very low, as low as 0.13 mA/cm^2.

The plating temperature was 65°C. The total plating time was 28 min. The process was stopped for stirring every 7 min to make the coating more homogeneous.

(d) *Removing the remaining electrolyte from the filaments.* After plating, the filaments were separated from the electrolyte by vacuum filtration. Then the filaments were immersed in water at about 65°C and stirred to remove the remaining electrolyte. The uncoated filaments were washed away along with the electrolyte and water. Then vacuum filtration was conducted. This process was repeated for at least five times, or until the filtrate became totally clear and the uncoated filaments were absent.

(e) *Drying.* The filaments were dried in an oven at about 90 °C in air overnight.

For 1 g of carbon filaments, the weight of the final product was 7.4 g—much less than the amount of 76 g expected for perfect coverage of all the carbon filaments, due to the washing away of the uncoated filaments in step (d). Theoretically, the nickel's electrochemical equivalent quantity is, according to Faraday's Law, 1.095 g/A·h. In the above process, the theoretical yield should be 8.176 g. Hence, the efficiency of the process was 91%.

2.2. Scanning electron microscopy

SEM was used to observe the morphology of both nickel filaments and nickel fibers.

Fig. 2a and b show, at two magnifications, nickel fibers from National Standard Co. These fibers are about 300–800 μm long and 20 μm diameter. Each fiber is composed of two contacting parallel fibers of 20 μm in diameter. From Fig. 2a, it could be seen that the grains of the fiber are about 2–6 μm in size. There are many pores of about 1 μm size in the grain boundaries. These pores are expected to cause low strength and low electrical conductivity.

Fig. 3a and b show, at two magnifications, nickel fibers from Ribtec, Inc. These fibers have an irregular cross-sectional shape and their diameter range from 0.5 to 3 μm. Since it is hard to find both ends of a single fiber, it is expected that the length of the fibers is larger than 150 μm, which is the size of the photographed area. According to the manufacturer, the fiber length is 2000 μm. From Fig. 3a, it can be seen that there are many secondary fibers on a primary fiber. These secondary fibers can bridge between primary fibers to increase the electrical conductivity of fiber compacts and of fiber polymer-matrix composites.

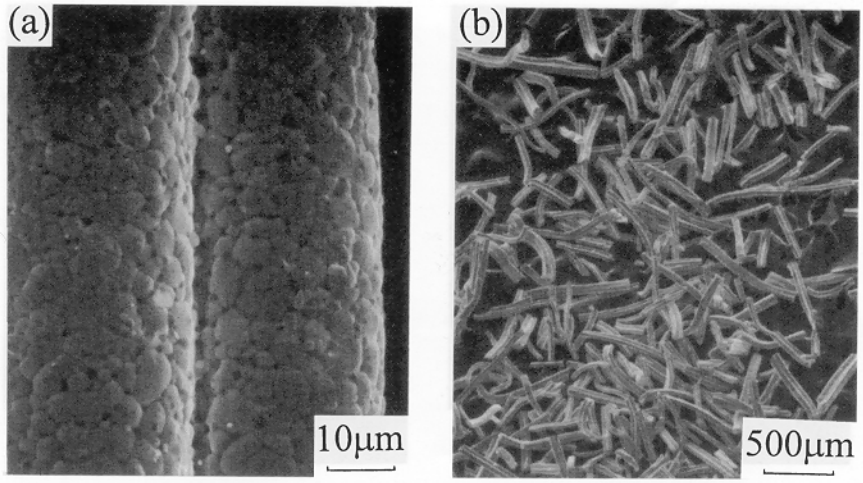

Figure 2 SEM photographs of 20 μm nickel fibers at two magnifications.

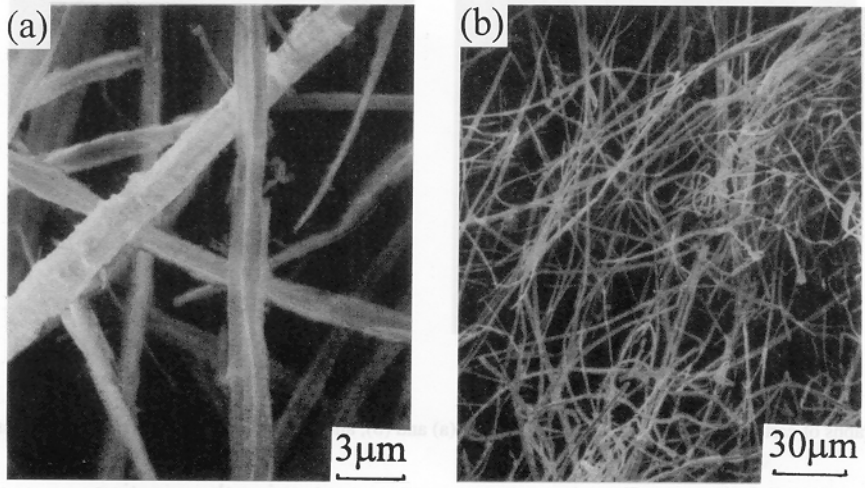

Figure 3 SEM photographs of 2 μm nickel fibers at two magnifications.

Fig. 4a and b shows, at two magnifications, the carbon filaments before electroplating. Fig. 4c and d show, at two magnifications, nickel filaments fabricated by coating nickel on the carbon filaments. Fig. 4c shows that all the filaments were coated with nickel homogeneously. No bare carbon filament could be found. Fig. 4d shows that the filament diameter is about 0.4 μm. It should be noticed that after coating, two crossing carbon filaments joined together at their junction. Such joints are desirable for increasing the electrical conductivity.

In order to obtain the nickel content of the nickel filaments, four SEM photographs each were taken for both carbon filaments and nickel filaments at a magnification of 30,000. Ten filaments were randomly chosen from each photograph to measure the diameter, so that each type of filament had 40 filaments measured. The average diameter of carbon filaments is 0.096 ± 0.018 μm. The average diameter of nickel filaments is 0.404 ± 0.022 μm. Thus, it could be calculated that the volume fraction of the carbon core is 5.6%, and the volume fraction of nickel is 94.4%.

The density $D_{\text{nickel filaments}}$ of the nickel filaments was calculated from the densities D and volume fractions V of the components by the Rule of Mixtures as

$$\begin{aligned} D_{\text{nickel filaments}} &= D_{\text{carbon filaments}} V_{\text{carbon filaments}} \\ &\quad + D_{\text{nickel}} V_{\text{nickel}} \\ &= (2 \times 0.056 + 8.9 \times 0.944)\ \text{g/cm}^3 \\ &= 8.51\ \text{g/cm}^3 \end{aligned}$$

The surface area of the nickel filaments were calculated by omitting the ends and joints. Since the surface area for one filament is $S = 2\pi rl$, and the volume of one filament is $\pi r^2 l$, the surface area of a unit volume is $2/r$ cm^2 and the surface area per unit weight is $2/rD$. Thus, the surface area of the nickel filaments is 1.16 m^2/g.

2.3. Electrical resistivity

Due to the small diameter of the carbon filaments, single filament electrical resistivity measurement was impossible. Thus, the electrical resistivity of filaments was estimated by measuring the electrical resistance of a filament compact. The four-point probe method was used. The testing fixture was made of steel and is shown in Fig. 5. The design incorporates a rectangular cavity into which the carbon filaments were placed and

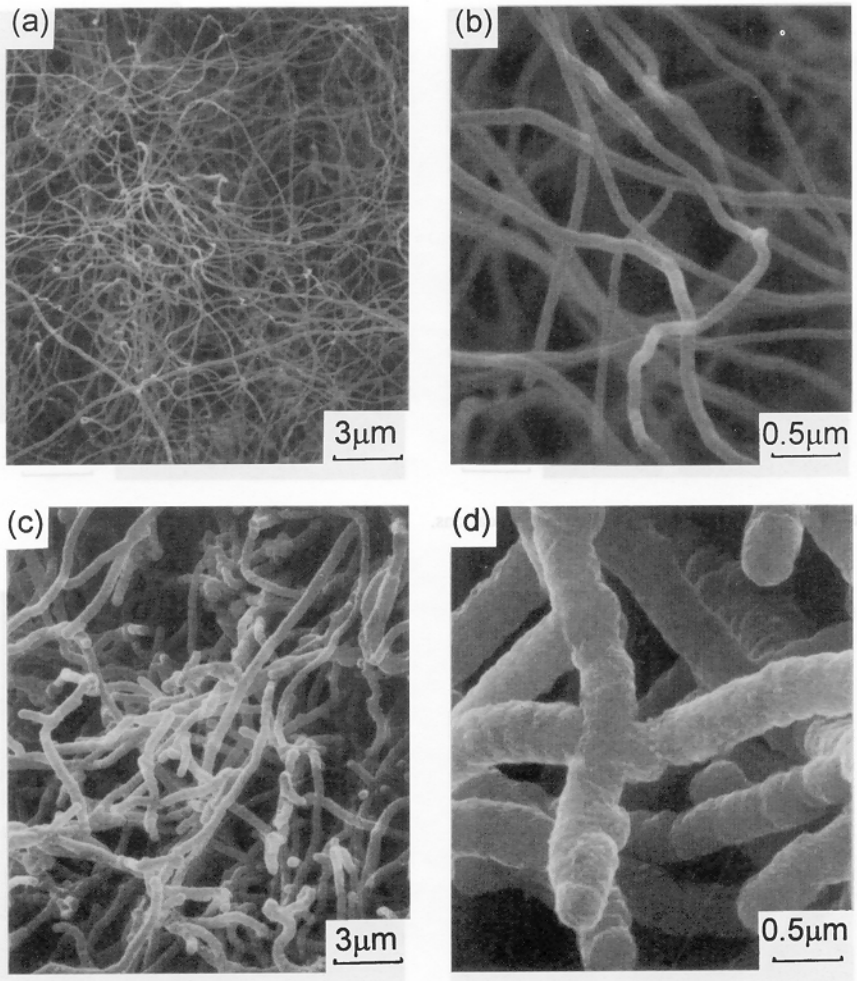

Figure 4 SEM photographs of carbon filaments at two magnifications, (a) and (b), and nickel filaments at two magnifications, (c) and (d).

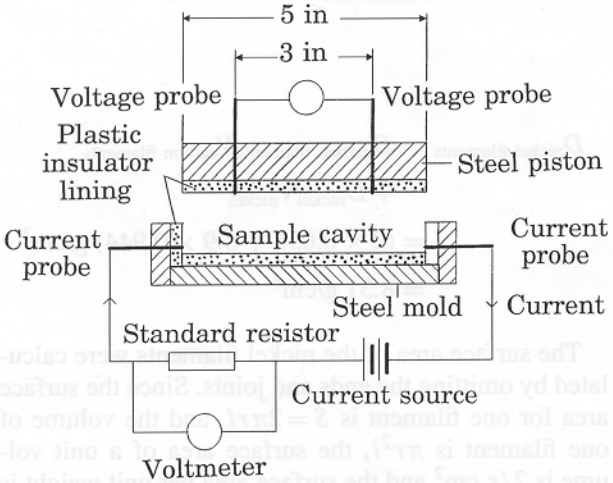

Figure 5 Set-up for four-probe electrical resistivity measurement of a compact.

compacted using a rectangular piston at a controlled pressure. Secured to the ends of the mold were probes (5 inches apart) used to pass current. Attached to the steel piston were two more probes placed at a fixed distance ($\ell = 3$ inches) apart. The potential developed across these two probes was measured as current was passed through the end probes. The compact electrical resistivity (ρ) was determined as a function of the cross sectional area A of the sample, which is a function of the piston position, and the potential drop, ΔV, between the probes for a known current, I, through the compact, using the equation

$$\rho = \left(\frac{\Delta V}{I}\right)\left(\frac{A}{l}\right) \tag{1}$$

The compacting pressure is directly proportional to the contact pressure between filaments for a given filament geometry. It is well known that the contact resistivity decreased with increasing contact pressure for electrical contacts in general. By increasing the pressure on the piston, the electrical resistivity gradually leveled off, as shown in Fig. 6. At a pressure of 7 MPa, the

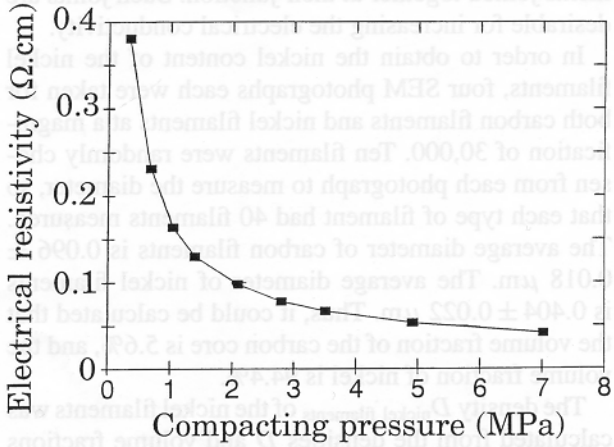

Figure 6 Electrical resistivity of carbon filament compact at different pressures.

resistivity of the as- received carbon filament compact is 0.041 Ω·cm.

A simple model to estimate the filament resistivity is based on the Rule of Mixtures. If, in the compact, all filaments are straight and aligned in one direction, the compact conductivity in the filament direction can be expressed as

$$\sigma_c = \sigma_f V_f + \sigma_m V_m, \tag{2}$$

where σ_c is the compact conductivity, σ_f is the filament conductivity, σ_m is the matrix conductivity, and V_f is the filament volume fraction and V_m is the matrix volume fraction.

In this case, the matrix is air. Thus σ_m is assumed to be zero. Thus Equation 2 can be written as

$$\sigma_c = \sigma_f V_f \tag{3}$$

or

$$\rho_f = \rho_c V_f \tag{4}$$

where ρ_f is the filament resistivity and ρ_c is the compact resistivity.

Since this model assumes that all filaments are straight and aligned in one direction, the σ_c is the highest possible value for a given σ_f. In other words, the ρ_f is the upper limit value for a given σ_c.

The second model to estimate the compact conductivity assumes that the conducting medium comprises straight short fibers randomly distributed in three-dimensional space [7]. Assuming that the angle between the axis of any short fiber and the current direction is θ, the possibility for a fiber to be in a direction between θ and $\theta + \delta\theta$ in three-dimensional space is $\sin\theta(\delta\theta/2)$ (Appendix A). The effective material contributing to conduction is reduced by a factor of $\cos^2\theta$ because the conducting fiber is not parallel to the current direction. Thus, the geometric factor g can be calculated by the equation

$$\begin{aligned} g &= \frac{2}{\pi/2}\int_0^{\pi/2} \cos^2\theta \sin\theta \, d\theta/2 \\ &= \frac{2}{\pi}\int_0^{\pi/2} \cos^2\theta \sin\theta \, d\theta \\ &= \frac{2}{3\pi} \end{aligned} \tag{5}$$

Hence, Equation 3 becomes

$$\sigma_c = \frac{2}{3\pi}\sigma_f V_f \tag{6}$$

or

$$\rho_f = \frac{2}{3\pi}\rho_c V_f \tag{7}$$

This three-dimensionally random distribution model is the other extreme compared to the Rule of Mixtures, which requires one-dimensional alignment of the conducting units. In the three-dimensional model, all the conducting units are randomly distributed in three-dimensional space and every conducting unit contributes to the conduction of the compact, such that there is no dead end for each unit electrically. Thus, σ_c is the lower limit for a given σ_f. In other words, ρ_f is the lower limit for a given σ_c.

In the experiments described above, the filaments were compressed by the piston to form two-dimensionally aligned layers. Similarly, the possibility of a fiber layer to be oriented between θ and $\theta + \delta\theta$ in two-dimensional space is $\delta\theta/2\pi$ (Appendix B). A two-dimensional model could be derived by calculating the geometric factor g as

$$\begin{aligned} g &= \frac{4}{\pi/2}\int_0^{\pi/2} \cos^2\theta \, d\theta/2\pi \\ &= \frac{4}{\pi^2}\int_0^{\pi/2} \cos^2\theta \, d\theta \\ &= \frac{1}{\pi} \end{aligned} \tag{8}$$

Thus, Equation 3 becomes

$$\sigma_c = \frac{1}{\pi}\sigma_f V_f \tag{9}$$

or

$$\rho_f = \frac{1}{\pi}\rho_c V_f \tag{10}$$

Equations 9 and 10 constitute a better approach to modeling the fiber compact and therefore are more accurate than either Equations 4 or 7. In reality, however, the fibers in the compact are not in a perfectly two-dimensional configuration, so the actual resistivity of a single fiber should be lower than that calculated by using Equation 10, i.e., between the values obtained by using Equations 7 and 10, and depends on the real configuration. The measured electrical resistivity of carbon filament compacts are summarized in Table II.

Results obtained by using the three models are listed in Table III. The compact electrical resistivity values

TABLE II Electrical resistivity of carbon filament compacts at various pressures

Pressure (MPa)	Resistivity (Ω·cm)	Density (g/cm^3)
0.35	0.38	0.16
0.70	0.23	0.20
1.1	0.16	0.24
1.4	0.13	0.27
2.1	0.098	0.33
2.8	0.078	0.37
3.5	0.067	0.41
4.9	0.053	0.47
7.0	0.041	0.56

TABLE III Electrical resistivity ρ_f of carbon filament estimated from the measured resistivity ρ_c of filament compact by three models

ρ_c (Ω·cm)	V_f	$\rho_f = \rho_c V_f$ (Ω·cm)	$\rho_f = \frac{1}{\pi}\rho_c V_f$ (Ω·cm)	$\rho_f = \frac{2}{3\pi}\rho_c V_f$ (Ω·cm)
0.041	0.281	0.0115	0.0037	0.0024

listed in Table III are values obtained under a 7 MPa compacting pressure and the filament volume fractions were calculated by using the density values of Table II at the same pressure.

The electrical resistivities of nickel fibers and nickel filaments were similarly measured on fiber/filament compacts. Electrical resistivity data obtained at different pressures are shown in Figs 7–9. The resistivity ρ_c of a fiber/filament compact at a pressure of 7 MPa was used to calculate the electrical resistivity of the fiber/filament. Three models were used to calculate the electrical resistivity, as shown in Table IV. The electrical resistivity of the 0.4 μm diameter nickel filaments is close to that of the 2 μm diameter nickel fibers, but much lower than that of the 20 μm diameter nickel fibers. The high resistivity of the 20 μm diameter nickel fibers is attributed to the pores. From Table IV, the resistivity of a nickel filament is between 4.3×10^{-6} and 6.5×10^{-6} Ω·cm. In contrast, from Table III, the resistivity of a carbon filament is between 2×10^{-3} and 4×10^{-3} Ω·cm.

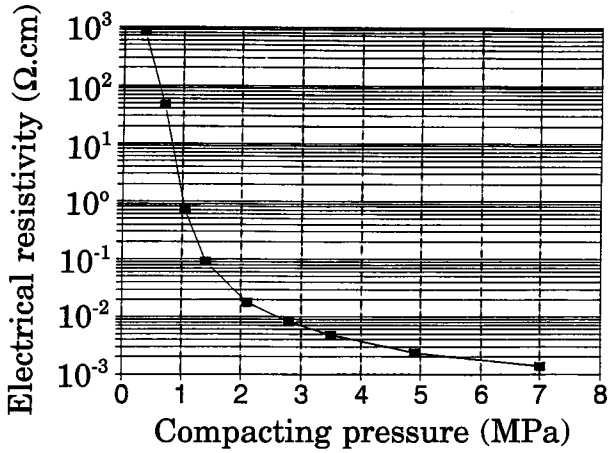

Figure 7 Electrical resistivity of 20 μm nickel fiber compact.

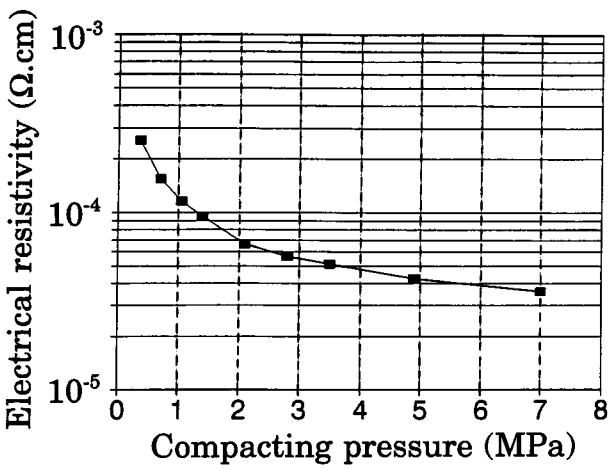

Figure 8 Electrical resistivity of 2 μm nickel fiber compact.

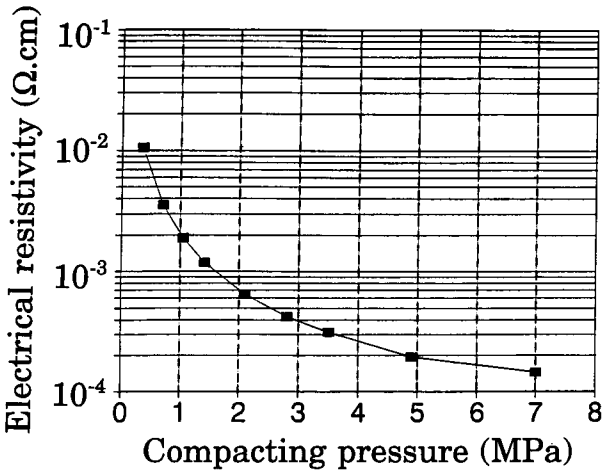

Figure 9 Electrical resistivity of nickel filament compact.

2.4. X-ray diffraction

X-ray diffraction was conducted using a Nicolet powder diffractometer system and Cu K_α radiation to examine the crystallographic nature of the fibers and filaments. The 2θ scan rate was 0.2° s^{-1}. It was found that the 20 μm nickel fiber has a sharp and narrow (111) peak, indicating a large crystal size. The x-ray diffraction patterns of the 2 μm nickel fiber and the 0.4 μm nickel filaments show broadening of the (111) peak, indicating smaller grain sizes.

To calculate the grain size of the nickel fibers and filaments, the full-width-at-half-maximum B of the (111) nickel peak of nickel fibers and filaments was measured and corrected by using Warren's method:

$$B^2 = B_m^2 + B_s^2 \tag{11}$$

where B is the corrected full-width-at-half-maximum, B_m is the full-width-at-half-maximum of the sample to be measured, and B_s is the full-width-at-half-maximum of the standard.

The 20 μm nickel fibers was used as a standard since, from SEM photograph of Fig. 2, it was known that the grain size is about 2–6 μm, large enough to be used as a standard in Warren's method. The grain size is then

$$t = \frac{0.9\lambda}{B\cos\theta} \tag{12}$$

where λ is the wavelength of Cu K_α radiation, which is 1.5418 Å, θ is the diffraction angle, and B is the corrected full-width-at-half-maximum.

TABLE IV Electrical resistivity ρ_f of nickel fiber/filament estimated from the measured resistivity ρ_c of fiber/filament compact by three models

Fiber/filament	ρ_c Ω·cm	V_f	$\rho_f = \rho_c V_f$ (Ω·cm)	$\rho_f = \frac{1}{\pi}\rho_c V_f$ (Ω·cm)	$\rho_f \frac{2}{3\pi}\rho_c V_f$ (Ω·cm)
20 μm nickel fiber	1.4×10^{-3}	0.372	5.21×10^{-4}	1.66×10^{-4}	1.11×10^{-4}
2 μm nickel fiber	7.35×10^{-5}	0.259	1.90×10^{-5}	6.06×10^{-6}	4.04×10^{-6}
0.4 μm nickel filaments	1.44×10^{-4}	0.142	2.04×10^{-5}	6.51×10^{-6}	4.34×10^{-6}

TABLE V Grain sizes of the nickel fibers and filaments

Fiber diameter (μm)	Grain size (μm)
20	2
2	0.018
0.4	0.016

The calculated grain size of the nickel fibers and filaments are listed in Table V. In spite of the large grain size, the 20 μm diameter nickel fibers exhibited a high electrical resistivity due to the pores. The 2 μm diameter nickel fibers and the 0.4 μm diameter nickel filaments are similar in both grain size and resistivity.

3. Composites

3.1. Composite fabrication

Polyether sulfone (PES), a thermoplastic provided as Victrex PES 4100P by ICI, was used as the matrix material. Its properties are shown in Table VI. The composites were fabricated by forming a mixture of the polymer powder and the filler and subsequent hot pressing in a steel mold at 310°C (processing temperature for PES, as recommended by ICI) and 13.4 MPa for about 30 min. For the nickel filaments and the 20 μm nickel fibers, the mixing was carried out dry in a ball mill for about 15 min. For carbon filaments, mixing was carried out wet—with water in a blender at a low speed, and then the wet mix was vacuum filtrated and dried at 120°C for at least 4 h. Due to the large length of the 2 μm nickel fibers (which resemble cotton wool), the dispersion of these fibers was most difficult. The mixing was performed by hand, as neither abovementioned dry mixing nor wet mixing was possible.

3.2. Mechanical properties

The samples for mechanical testing were of size 80 × 8 × 3 mm. End tabs were attached to both ends by epoxy. Strain gages were used to measure the strain. Testing was conducted by using a hydraulic materials testing system (MTS 810). The displacement rate was 1.0 mm/min. Hydraulic grips were used to grip the samples. Each filler was at four different volume fractions and each volume fraction involved four samples. Table VII summarizes the mechanical properties of composites with four kinds of filler at different volume fractions.

Fig. 10 shows that the tensile strength of the 2 μm nickel fiber PES-matrix composites increases with increasing filler volume fraction while the tensile strength of composites using other fillers decreases with increasing filler volume fraction. This indicates that the bonding between filler and polymer is poor for all fillers except the 2 μm nickel fiber. For the nickel filaments, the tensile strength remains unchanged up to 7 vol.% filaments. Above 7 vol.%, the tensile strength decreases 1.8 MPa (or 3.5% of total strength) per volume percent of filaments added.

Fig. 11 shows that the Young's modulus of all composites increases with increasing filler volume. The modulus of composites using nickel filaments increases linearly with increasing filament volume fraction.

Fig. 12 shows that the tensile ductility of all composites decreases with increasing filler volume fraction.

TABLE VI Properties of polyether sulfone polymer

T_g	220–222°C
Density	1.37 g/cm^3
Particle size	100–150 μm
Tensile strength	45.93 ± 1.12 MPa
Tensile modulus	2.64 ± 0.19 GPa
Elongation at break	(3.1 ± 0.3)%
Electrical resistivity	>10^{10} Ω·cm
Coefficient of thermal expansion	55 × 10^{-6}/K

TABLE VII Mechanical properties of PES-matrix composites

Filler	Volume %	Strength (MPa)	Modulus (GPa)	Strain at break (%)
Nickel filaments	0	53.0 ± 2.3	2.7 ± 0.1	2.1 ± 0.1
	3	53.0 ± 2.3	3.8 ± 0.1	1.45 ± 0.05
	7	51.5 ± 3.1	5.2 ± 0.2	1.01 ± 0.04
	13	38.2 ± 2.1	7.2 ± 0.1	0.55 ± 0.02
	19	30.3 ± 0.6	9.1 ± 0.1	0.33 ± 0.01
2 μm nickel fiber	0	53.0 ± 2.3	2.7 ± 0.1	2.1 ± 0.1
	3	60.2 ± 2.4	4.7 ± 0.5	1.73 ± 0.15
	7	65.6 ± 7.1	6.1 ± 0.3	1.52 ± 0.06
	13	81.8 ± 2.3	9.8 ± 1.3	1.00 ± 0.18
	19	66.1 ± 6.5	11.9 ± 1.5	0.58 ± 0.09
20 μm nickel fiber	0	53.0 ± 2.3	2.7 ± 0.1	2.1 ± 0.1
	19	53.0 ± 0.6	6.8 ± 0.6	1.47 ± 0.15
	25	42.5 ± 2.1	8.5 ± 0.8	0.59 ± 0.04
	37	39.9 ± 2.4	14.8 ± 3.2	0.32 ± 0.01
	43	34.6 ± 3.4	14.6 ± 0.6	0.30 ± 0.01
Carbon filaments	0	53.0 ± 2.3	2.7 ± 0.1	2.1 ± 0.1
	3	50.4 ± 2.4	3.2 ± 0.1	1.34 ± 0.05
	7	47.6 ± 3.4	3.8 ± 0.1	1.30 ± 0.03
	13	36.3 ± 2.1	4.1 ± 0.06	0.98 ± 0.05
	19	27.7 ± 0.8	4.4 ± 0.03	0.67 ± 0.02

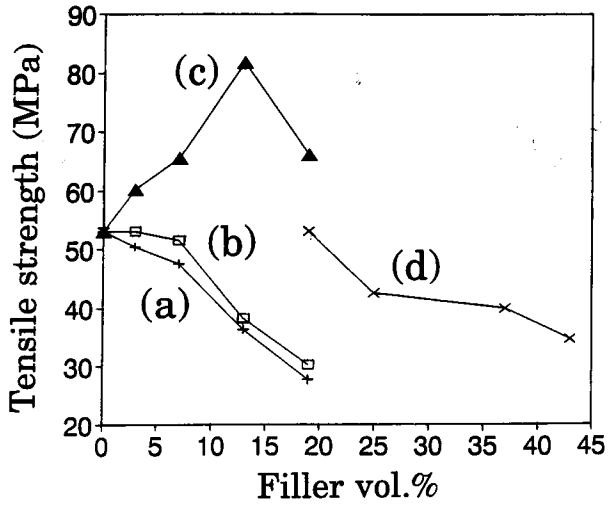

Figure 10 Tensile strength of PES-matrix composites. (a) Carbon filaments (+). (b) Nickel filaments (□). (c) 2 μm nickel fibers (▲). (d) 20 μm nickel fibers (×).

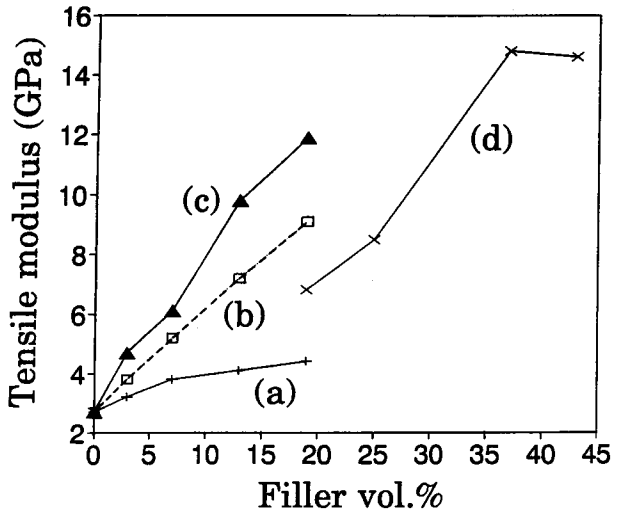

Figure 11 Tensile modulus of PES-matrix composites. (a) Carbon filaments (+). (b) Nickel filaments (□). (c) 2 μm nickel fibers (▲). (d) 20 μm nickel fibers (×).

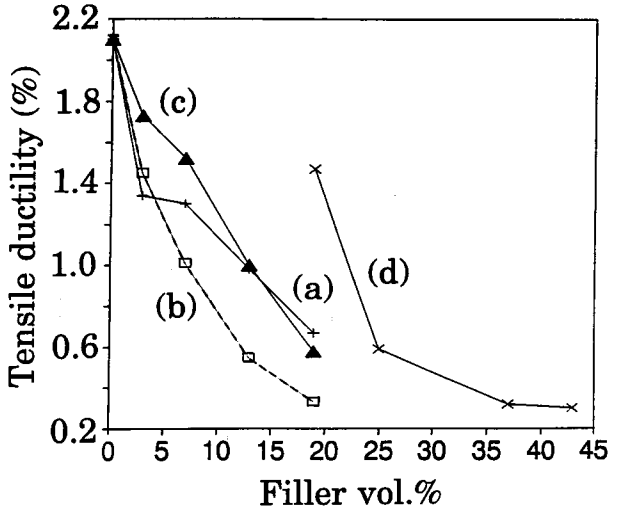

Figure 12 Tensile ductility of PES-matrix composites. (a) Carbon filaments (+). (b) Nickel filaments (□). (c) 2 μm nickel fibers (▲). (d) 20 μm nickel fibers (×).

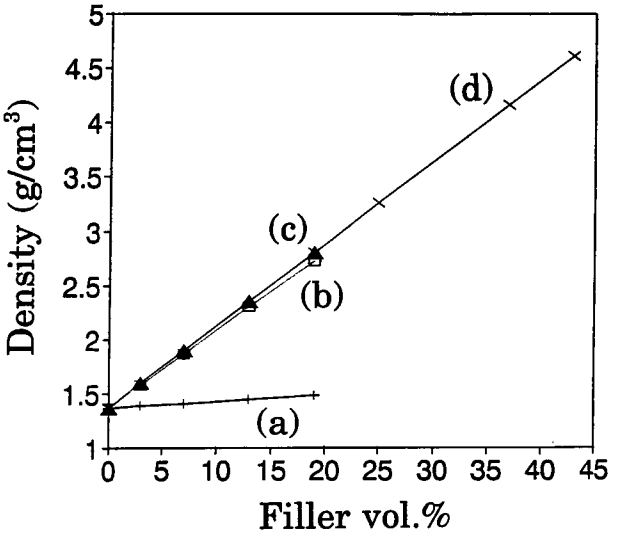

Figure 13 Density of PES-matrix composites. (a) Carbon filaments (+). (b) Nickel filaments (□). (c) 2 μm nickel fibers (▲). (d) 20 μm nickel fibers (×).

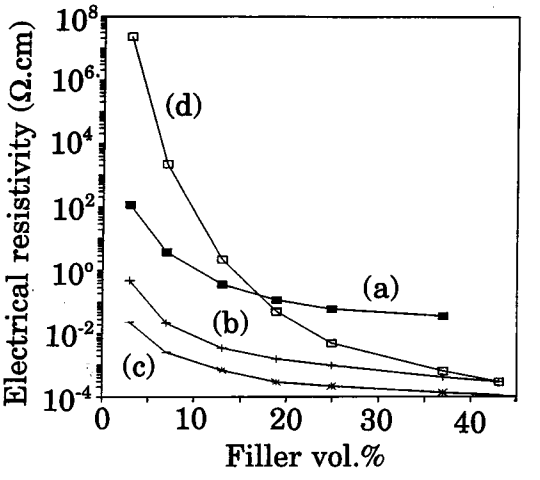

Figure 14 Electrical resistivity of PES-matrix composites. (a) Carbon filaments (■). (b) Nickel filaments (+). (c) 2 μm nickel fibers (*). (d) 20 μm nickel fibers (□).

The ductility of composites using nickel filaments decreases most dramatically. This is probably due to the deformation constraint caused by the quasi three-dimensional network which was formed during nickel plating, as shown in Fig. 4d. Fig. 13 shows that carbon filaments PES-matrix composites have the lowest density among all the composites studied.

3.3. Electrical resistivity

The electrical resistance R was measured using the four-probe method. Silver paint was used for the electrical contacts. The four probes consisted of two outer current probes and two inner voltage probes. The resistance R refers to the sample resistance between the inner probes. The distance between the inner probes was 50 mm. The samples were of size 80 × 4 × 3 mm. The current (dc) used was controlled at about 1 mA.

Fig. 14 shows the electrical resistivity of composites using different fillers. The 2 μm nickel fiber composites have the lowest resistivity while the 20 μm nickel fiber composites have the highest resistivity at a low filler volume fraction. At a high filler volume fraction, all the three nickel fiber/filament composites have resistivity 10^{-4} Ω·cm. The lowest resistivity of the carbon filament composites is 10^{-2} Ω·cm; this high value is due to the poor conductivity of carbon filament compared to the nickel fiber/filament. At low filler volume fractions, the electrical resistivities of composites with different fillers have larger differences, but at high volume fractions, the resistivities tend to be close. The 2 μm nickel fiber composites have the lowest electrical resistivity at all fiber volume fractions due to less defects (compared to the 20 μm diameter nickel fibers) and less contacts (compared to the 0.4 μm diameter nickel filaments).

3.4. EMI shielding effectiveness and reflection coefficient

The EMI shielding effectiveness was measured by an HP-8510A Network Analyzer using the coaxial cable method, as shown in Fig. 15. The sample was in the form of an annular ring of outer diameter 97 mm and inner diameter 32 mm. Silver paint was used to paint

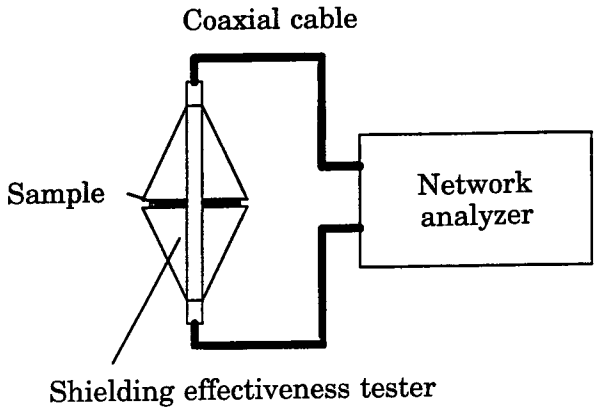

Figure 15 Schematic of an EMI shielding effectiveness measurement set-up.

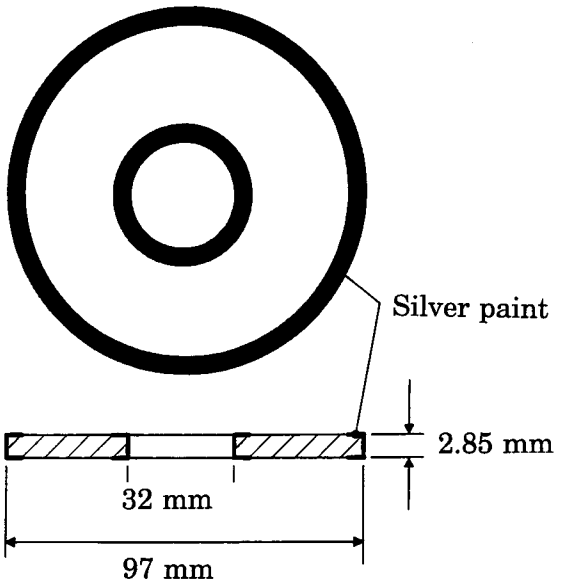

Figure 16 Testing sample configuration for EMI shielding effectiveness measurement.

the edge of the sample, as illustrated in Fig. 16. The sample thickness was 2.85 mm for all the composites, 3.1 mm for solid copper, 3.0 mm for solid nickel, and 4.0 mm for solid stainless steel. The sample was held by an Elgal SET 19A (Israel) shielding effectiveness tester, as shown in Fig. 15, which, due to its geometry, theoretically allowed testing at frequencies up to 1.5 GHz. Since the main interest in this work was to test EMI shielding effectiveness at gigahertz frequency range, a broader range of EMI shielding effectiveness from 0.5 GHz to 3 GHz was tested using a copper standard sample. The testing result showed that, although the theoretical allowable testing frequency range is up to 1.5 GHz, the actual measured EMI shielding effectiveness of a copper standard sample from 0.5 GHz to 3 GHz only varied within ±5 dB. The EMI shielding effectiveness value we dealt with in this work is already at the upper measurement limit of this equipment (80–100 dB) and an error ±5 dB is unavoidable. Therefore, a testing frequency range of 1–2 GHz was chosen in this work.

Prior to the tests, the measurement system was calibrated by using a Hewlett-Packard APC-7 Calibration Kit. The calibration was conducted using the two ports-one pass method, with an average of 128 points. Isolation was also calibrated to reduce the noise at high attenuation. An HP computer using HP BASIC 2.0 was connected to the HP-8510A to acquire data.

The frequency was scanned from 1 to 2 GHz at 10 MHz intervals such that 101 data points were taken within this frequency range. To test the EMI shielding effectiveness of the shielding materials, the shielding effectiveness tester was first tested without a sample to get the baseline data. The baseline was less than 1 dB and was subtracted from the measured EMI shielding effectiveness of the sample.

It was found that the amount of torque applied on the bolts used to fasten together the two halves of the shielding effectiveness tester has significant effect on the test results. If the torque is not large enough, the shielding effectiveness value will be significantly lower than the actual value. To evaluate the impact of the amount of torque to the shielding effectiveness results, a series of tests was done using a 4 mm thick stainless steel standard sample at various values of the torque. The results are listed in Table VIII. The shielding effectiveness increases with the torque, such that it stabilizes when the torque exceeds 12 in·lb. Thus, a torque of 14 in·lb was chosen in all the experiments.

The shielding effectiveness of four types of PES-matrix composites with different filler materials, namely nickel filaments, 2 μm diameter nickel fibers, 20 μm diameter nickel fibers and carbon filaments, were tested. Within each type of composite, four different filler contents were used. By following the experimental procedure described above, 101 data from 1 to 2 GHz were collected for each sample. The average of these 101 data for each sample is shown in Table IX, together with the standard deviation of these 101 data. Figs 17–21 give all the data for each composite sample as well as solid copper, nickel and stainless steel. The error of each data point was better than ±1 dB at <10 dB, and ±5 dB at >70 dB. The error increased with increasing attenuation (dB).

Table IX shows that, at the same filler volume fraction, the shielding effectiveness was the highest for the nickel filaments. At 7 vol.%, the advantage of the nickel filaments compared to the other filaments was most significant. The shielding effectiveness attained by nickel filaments at 7–19 vol.% was comparable to those of solid metals, such as copper, nickel and stainless steel, which were even thicker than the composites. Even at 43 vol.%, the 20 μm diameter nickel fibers gave lower shielding effectiveness than the nickel filaments

TABLE VIII The effect of torque on EMI shielding effectiveness results

Torque (in·lb)	EMI shielding effectiveness (dB)
4	52.3 ± 6.6
6	65.4 ± 4.5
8	75.1 ± 2.5
10	82.4 ± 3.7
12	88.7 ± 4.2
14	88.9 ± 4.0
16	89.1 ± 4.3

TABLE IX EMI shielding effectiveness (dB) averaged in the range 1–2 GHz

Filler vol.%	0.4 μm Ni filaments/ PES composites	Carbon filaments/ PES composites	2 μm Ni fibers/ PES composites	20 μm Ni fibers/ PES composites
3	42.2 ± 2.4	20.6 ± 1.3	45.2 ± 2.5	
7	86.6 ± 5.1	31.8 ± 1.7	58.1 ± 4.2	
13	83.7 ± 5.3	53.6 ± 3.5	60.3 ± 3.2	
19	91.7 ± 6.6	73.9 ± 5.1	71.7 ± 4.6	4.9 ± 1.9
25				10.5 ± 2.3
37				38.4 ± 1.9
43				73.7 ± 4.4
Solid copper	90.2 ± 5.0			
Solid nickel	82.1 ± 6.8			
Solid stainless steel	88.9 ± 4.0			

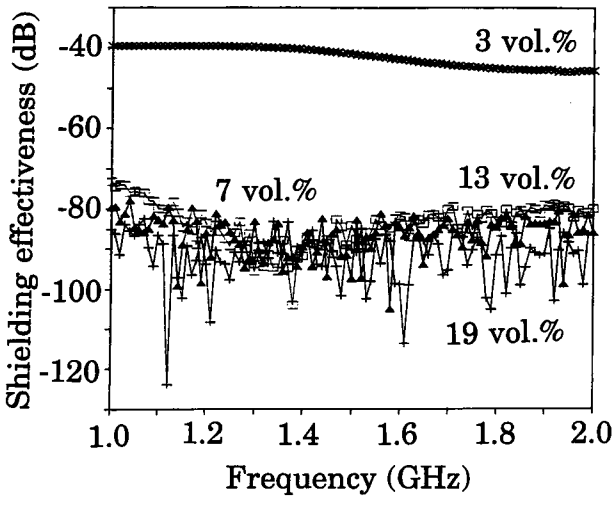

Figure 17 EMI shielding effectiveness of 0.4 μm nickel filaments/PES composites at frequency range from 1 to 2 GHz and nickel filament volume fraction 3% (×), 7% (▲), 13% (□) and 19% (+).

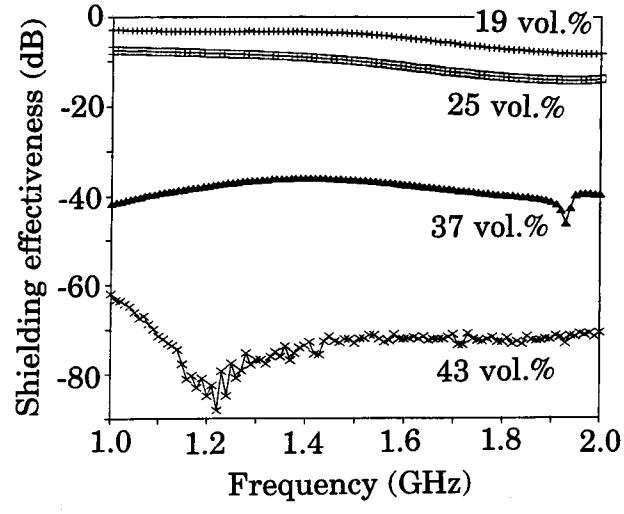

Figure 19 EMI shielding effectiveness of 20 μm nickel fiber/PES composites at frequency range from 1 to 2 GHz and nickel fiber volume fraction 19% (+), 25% (□), 37% (▲) and 43% (×).

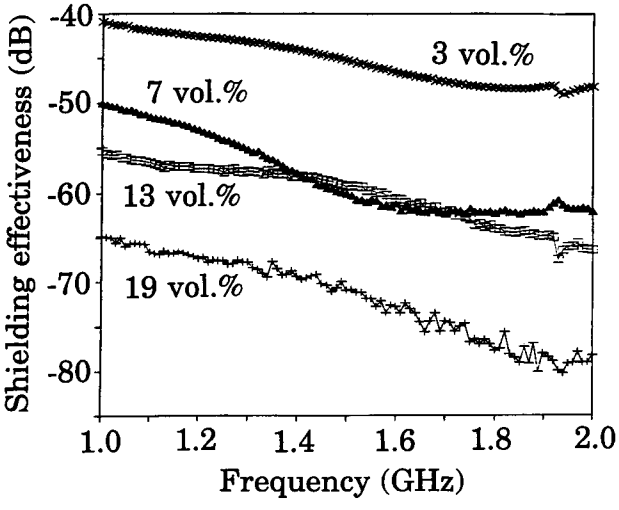

Figure 18 EMI shielding effectiveness of 2 μm nickel fiber/PES composites at frequency range from 1 to 2 GHz and nickel fiber volume fraction 3% (×), 7% (▲), 13% (□) and 19% (+).

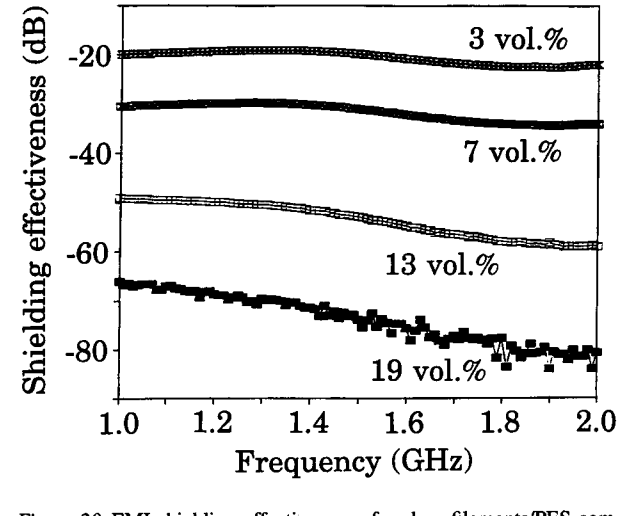

Figure 20 EMI shielding effectiveness of carbon filaments/PES composites at frequency range from 1 to 2 GHz and carbon filament volume fraction 3% (⧖), 7% (⊠), 13% (□) and 19% (■).

at 7 vol.%. Even at 19 vol.%, the 2 μm diameter nickel fibers and the carbon filaments gave lower shielding effectiveness than nickel filaments at 7 vol.%. The high shielding effectiveness associated with the nickel filaments is attributed to the combination of small diameter (smaller than the nickel fibers) and low electrical resistivity (lower than all except the 2 μm diameter nickel fibers) of the nickel filaments.

For plane electromagnetic waves at high frequencies, the shielding effectiveness SE of a barrier (i.e., effectiveness in reducing the energy of an incident electromagnetic field) can be computed as the sum of three terms, each representing one of the loss phenomena,

TABLE X Theoretical values of reflection loss and absorption loss at 1.5 GHz for selected materials

Material	Reflection loss (dB)	Absorption loss (dB)
PES-matrix composite with 3 vol.% nickel filaments	1.5	261.0
PES-matrix composite with 7 vol.% nickel filaments	15.1	1244.4
PES-matrix composite with 13 vol.% nickel filaments	23.0	3119.9
PES-matrix composite with 19 vol.% nickel filaments	26.7	4765.7
Solid copper	76.2	14249.5
Solid nickel	50.0	69798.2

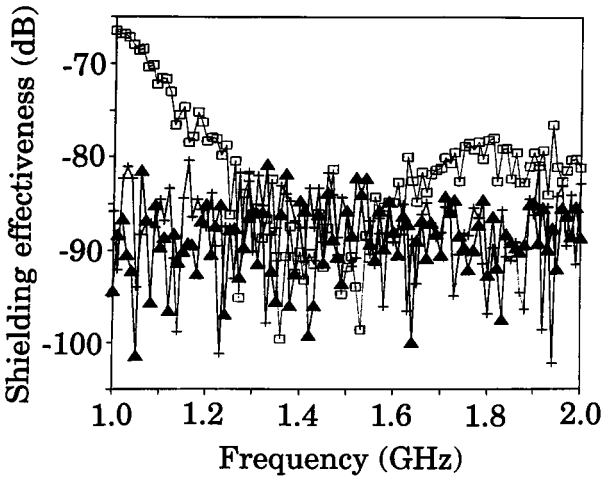

Figure 21 EMI shielding effectiveness of solid copper (+), nickel (□) and stainless steel (▲) plate at frequency range from 1 to 2 GHz.

i.e., reflection loss, absorption loss, and multiple reflections.

$$SE = R + A + M \tag{13}$$

where R represents the reflection loss at the interface at which the incident wave hits the barrier, A represents the absorption loss of the wave as it proceeds through the barrier, and M represents the additional effects of multiple reflections and transmissions.

For plane waves, the reflection loss [8] in dB is

$$R(\text{dB}) = 168 + 10\log_{10}\left(\frac{\sigma_r}{\mu_r f}\right) \tag{14}$$

where μ_r is the relative permeability of the barrier metal, σ_r is the conductivity relative to copper, and f is the frequency in Hz.

For plane waves the absorption loss in dB is

$$A(\text{dB}) = 131.4\, t\sqrt{f\mu_r\sigma_r} \tag{15}$$

where t is the thickness of the barrier in meters.

Theoretical values for the reflection loss R (dB) and the absorption loss A (dB) were calculated using Equations 14 and 15 and are given in Table X. Note that the values for R (dB) are less than the SE (dB) values listed in Table IX for all the materials. Note also that the A(dB) values are far in excess of what were measured. It is believed that this may indicate a leakage path around the test specimen because clearly the electromagnetic waves propagating directly through the test specimen is completely absorbed.

The shielding effectiveness of the composite with 13 vol.% carbon filaments is higher than that of the composite with ~45 vol.% carbon filaments reported in Ref. 9. This difference is attributed to the difference in composite processing and to the difference in the carbon filaments used in this work and in Ref. 9.

Table XI shows the reflection coefficient S_{11} (ratio of the amplitude of reflected wave to that of incident wave) for the samples. It should be noted that the effects of test fixture reflections had not been eliminated. The values in Table XI indicate that most of the power incident upon the sample was reflected. As discussed previously in relation to Table X, any power penetrating the test specimen is absorbed. At the same filler volume fraction, the reflection coefficient was highest for the nickel filaments. At 7 and 13 vol.%, the advantage of the nickel filaments compared to the other fillers was most significant. The reflection coefficient attained by nickel filaments at 7–19 vol.% was comparable to those of solid metals, such as copper, nickel and stainless steel. The high reflection coefficient indicates a high surface electrical conductance.

Table XII compares the EMI shielding effectiveness at 1–2 GHz of PES-matrix composites with various fillers at the same sample thickness of 2.8 mm. The shielding effectiveness for all specimens was determined by the coaxial cable method using the same tester. Even at a low filler content of 7 vol.%, the nickel filaments provided much greater shielding

TABLE XI Reflection coefficient averaged in the range 1–2 GHz

Filler vol.%	0.4 μm Ni filaments/ PES composites	Carbon filaments/ PES composites	2 μm fibers/ PES composites	20 μm Ni fibers/ PES composites
3	0.908 ± 0.007	0.854 ± 0.022	0.933 ± 0.007	
7	0.953 ± 0.005	0.898 ± 0.008	0.947 ± 0.006	
13	0.964 ± 0.005	0.929 ± 0.007	0.951 ± 0.006	
19	0.957 ± 0.005	0.944 ± 0.006	0.957 ± 0.005	0.714 ± 0.084
25				0.800 ± 0.039
37				0.939 ± 0.012
43				0.964 ± 0.005
Solid copper	0.953 ± 0.005			
Solid nickel	0.961 ± 0.005			
Solid stainless steel	0.954 ± 0.007			

TABLE XII Electromagnetic interference shielding effectiveness at 1–2 GHz of PES-matrix composites with various fillers

Filler	Vol.%	EMI shielding effectiveness (dB)	Ref.
Al flakes ($15 \times 15 \times 0.5$ μm)	20	26	11
Steel fibers (1.6 μm dia. × 30–56 μm)	20	42	11
Carbon fibers (10 μm dia. × 400 μm)	20	19	11
Ni particles (1–5 μm dia.)	9.4	23	12
Ni fibers (20 μm dia. × 1 mm)[a]	19	5	This work
Ni fibers (2 μm dia. × 2 mm)[a]	7	58	This work
Carbon filaments (0.1 μm dia. × > 100μm)[a]	7	32	This work
Ni filaments (0.4 μm dia. × > 100 μm)[a]	7	87	This work

[a]Sample thickness ~2.8 mm.

effectiveness than all the other fillers of Table XII. In the case of the matrix being polyimidesiloxane (PISO) instead of PES, it has been shown that nickel particles of size 1–5 μm provide greater EMI shielding effectiveness at 1–2 GHz than silver particles of size 0.8–1.35 μm [10]. Together with Table XII, this means that nickel filaments provide greater shielding effectiveness than silver particles.

4. Discussion

The tensile strength (Fig. 10) decreased monotonically with increasing filler volume fraction for all the fillers except the 2 μm diameter nickel fibers, for which the strength increased with increasing filler volume fraction up to 13% and then decreased with further increase of the volume fraction. This means that the filler-matrix bonding was strongest for the 2 μm diameter nickel fibers, so that only these fibers were able to reinforce the composite. In all cases, the decrease of the strength with increasing filler volume fraction was due to the increase in void content with increasing filler content and the weak filler-matrix bonding. The modulus (Fig. 11) increased monotonically with increasing filler volume fraction for all the fibers. The ductility (Fig. 12) decreased monotonically with increasing filler volume fraction for all the fibers. The tensile strength was highest for composites with the 2 μm diameter nickel fibers and lowest for composites with carbon filaments (Fig. 10). The strength (Fig. 10) and modulus (Fig. 11) of the nickel filament composites were higher than those of the carbon filament composites, but lower than those of the 2 μm diameter nickel composites at the same corresponding filler volume fraction. The ductility (Fig. 12) was lower for the nickel filament composites than both the carbon filament composites and the 2 μm diameter nickel fiber composites at the same corresponding filler volume fractions from 7% to 19%. The clinginess (like cotton wool) of the nickel filaments and carbon filaments is believed to cause the ductility of these composites to be lower than those of the nickel fiber composites. The higher ductility (at 7–19 vol.%), lower modulus and lower strength of the carbon filament composites compared to the nickel filament composites are attributed to the smaller diameter and probably weaker filler-matrix bonding of the carbon filaments.

TABLE XIII Properties of the composite with the best overall (electrical and mechanical) performance for each filler type

	EMI shielding effectiveness (dB)	Tensile strength (MPa)	Tensile ductility (%)
7 vol.% nickel filaments	86.6	51.5	1.01
19 vol.% carbon filaments	73.9	27.2	0.67
19 vol.% 2 μm nickel fibers	71.7	66.1	0.58
43 vol.% 20 μm nickel fibers	73.7	34.6	0.3

TABLE XIV Specific EMI shielding effectiveness at 1–2 GHz for competing composites and solid copper. Standard deviations are shown in parentheses

Material	Specific EMI shielding effectiveness (dB·cm^3/g)
7 vol.% nickel filaments	47 (3)
19 vol.% carbon filaments	50 (4)
7 vol.% 2 μm nickel fibers	31 (3)
43 vol.% 20 μm nickel fibers	16 (5)
Copper	10 (0.5)

The carbon filament composites are advantageous over all the nickel composites in their low density (Fig. 13). Nevertheless, at a low filler volume fraction of 7%, the nickel filament composite's density was quite low (1.87 g/cm^3).

Although the nickel filament composites are not particularly attractive in ductility, strength or modulus than the other composites at the same filler volume fraction (at or above 7%), the nickel filaments are the only filler that gives simultaneously shielding effectiveness exceeding 70 dB, ductility >0.7% and strength >40 MPa, when all filler volume fractions are considered, as shown in Table XIII, which lists the composite with the best overall (electrical and mechanical) performance for each filler type.

Due to aerospace applications related to shielding or waveguides, the specific EMI shielding effectiveness (EMI shielding effectiveness divided by the density) is a relevant quantity, which is listed in Table XIV for the composites at the filler volume fraction that gives the highest shielding effectiveness in each of the four categories in Table XI. The specific shielding effectiveness was highest for both the composite with 19 vol.% carbon filaments and that with 7 vol.% nickel filaments. Compared to all composites of Table XIV, solid copper gave the lowest value for the specific shielding effectiveness.

5. Conclusion

A method was developed to fabricate nickel filaments of 0.4 μm diameter by electroplating nickel on carbon

filament. The nickel filament contained 94 vol.% of nickel and 6 vol.% of carbon core. Because of its small diameter, hence large surface area, the nickel filament is useful in many application areas. It is simple to fabricate in large quantities at low cost and to mix with polymer particles to make polymer-matrix composites. X-ray diffraction shows that the grain size of the 0.4 μm diameter nickel filaments was 16 nm.

Polyether sulfone (PES)-matrix composites using the submicron diameter nickel filaments as a filler were fabricated. The tensile strength of the nickel filament PES-matrix composites remained unchanged up to 7% filament volume fraction. Above 7 vol.%, the strength of the nickel filament PES-matrix composites decreased significantly. The electrical resistivity of the nickel filament PES-matrix composite was comparable to that of a 2 μm diameter nickel fiber PES-matrix composite at the same filler volume fraction, and lower than that of a 20 μm diameter nickel fiber PES-matrix composite and that of a carbon filament PES-matrix composite at the same filler volume fraction.

The submicron diameter nickel filament PES-matrix composites were found to exhibit exceptionally high EMI shielding effectiveness due to their high reflectivity at 1–2 GHz at filler volume fractions as low as 7%. The shielding effectiveness and surface impedance achieved with 7 vol.% nickel filaments were 87 dB and 1.2 Ω respectively—both comparable to those of solid copper. The excellent properties of the nickel filaments for EMI shielding are attributed mainly to the combination of high electrical conductivity, ferromagnetic nature [2], exceptionally small diameter and large aspect ratio.

Appendix A

The volume δV from θ to $\theta + \delta\theta$ of unit length fiber is

$$\delta V = 2\pi \int_0^1 \int_\theta^{\theta+\delta\theta} r^2 \sin\phi \, dr \, d\phi$$

$$= \frac{2\pi}{3}[\cos\theta - \cos(\theta + \delta\theta)]$$

$$= \frac{2\pi}{3}[\cos\theta - (\cos\theta \cos\delta\theta - \sin\theta \sin\delta\theta)]$$

Since $\delta\theta$ is very small, $\cos\delta\theta \sim 1$ and $\sin\delta\theta \sim \delta\theta$. Thus, $\delta V \sim (2\pi/3)\,\delta\theta \sin\theta$.

Under the assumption of uniform distribution, the probability is proportional to the volume, so that

$$P = \frac{\delta V}{V} = \frac{(2\pi/3)\,\delta\theta \sin\theta}{(4\pi/3)} = \frac{1}{2}\,\delta\theta \sin\theta$$

Appendix B

The area δS from θ to $\theta + \delta\theta$ of unit length of fiber is $\delta S = \delta\theta/2$. Thus, the probability becomes $P = \delta S/S = \delta\theta/2\pi$.

Acknowledgement

This work was supported by Defense Advanced Research Projects Agency and Applied Sciences, Inc. Helpful discussion with Dr. Pay Yih of State University of New York at Buffalo concerning the electroplating set-up is gratefully acknowledged.

References

1. X. SHUI and D. D. L. CHUNG, *J. Electron. Mater.* **24**(2) (1995) 107.
2. *Idem., ibid.* **25**(6) (1996) 930.
3. J. A. E. BELL and G. HANSEN, Proc. 24th Int. SAMPE Technical Conf., 1992, p. T902.
4. G. B. PARK and D. A. FOSTER, Proc. 77th AESF Annual Technical Conf. (American Electroplaters and Surface Finishers Society, 1990) pt. 2, p. 1349.
5. Y. X. GAN, C. Q. CHEN and C. G. LI, *Science and Engineering of Composite Materials* **2**(4) (1993) 271.
6. X. SHUI, C. A. FRYSZ and D. D. L. CHUNG, *Carbon* **33**(12) (1995) 1681.
7. A. R. BLYTHE, "Electrical Properties of Polymers" (Cambridge University Press, Cambridge 1979) p. 126.
8. C. R. PAUL, "Introduction to Electromagnetic Compatability" edited by Kai Chang, (Wiley, 1992) p. 649.
9. M. KATSUMATA, H. YAMANASHI, H. USHIJIMA and M. ENDO, *SPIE Proc.*, 1993, edited by Vijay K. Varadan, Vol. 1916: Smart Materials, p. 140.
10. L. LI and D. D. L. CHUNG, *Composites* **22**(3) (1991) 211.
11. *Idem., ibid.* **25**(3) (1994) 215.
12. *Idem., Polymer Composites* **14**(6) (1993) 467.

Received 10 February 1997
and accepted 30 September 1999